



Dendritic Cells Require PINK1-Mediated Phosphorylation of BCKDE1 α to Promote Fatty Acid Oxidation for Immune Function

Farhan Basit¹ and I. Jolanda M. de Vries^{1,2*}

¹ Department of Tumor Immunology, Radboud University Medical Center, Radboud Institute for Molecular Life Sciences, Nijmegen, Netherlands, ² Department of Medical Oncology, Radboud University Medical Center, Nijmegen, Netherlands

Dendritic cell (DCs) activation by Toll-like receptor (TLR) agonist induces robust metabolic rewiring toward glycolysis. Recent findings in the field identified mechanistic details governing these metabolic adaptations. However, it is unknown whether a switch to glycolysis from oxidative phosphorylation (OXPHOS) is a general characteristic of DCs upon pathogen encounter. Here we show that engagement of different TLR triggers differential metabolic adaptations in DCs. We demonstrate that LPS-mediated TLR4 stimulation induces glycolysis in DCs. Conversely, activation of TLR7/8 with protamine-RNA complex, pRNA, leads to an increase in OXPHOS. Mechanistically, we found that pRNA stimulation phosphorylates BCKDE1 α in a PINK1-dependent manner. pRNA stimulation increased branched-chain amino acid levels and increased fatty acid oxidation. Increased FAO and OXPHOS are required for DC activation. PINK1 deficient DCs switch to glycolysis to maintain ATP levels and viability. Moreover, pharmacological induction of PINK1 kinase activity primed immunosuppressive DC for immunostimulatory function. Our findings provide novel insight into differential metabolic adaptations and reveal the important role of branched-chain amino acid in regulating immune response in DC.

OPEN ACCESS

Edited by:

Hubertus Hochrein,
Bavarian Nordic, Germany

Reviewed by:

Tomoko Hayashi,
University of California, San Diego,
United States
Eyal Amiel,
University of Vermont, United States

*Correspondence:

I. Jolanda M. de Vries
Jolanda.deVries@radboudumc.nl

Specialty section:

This article was submitted to
Antigen Presenting Cell Biology,
a section of the journal
Frontiers in Immunology

Received: 22 July 2019

Accepted: 23 September 2019

Published: 15 October 2019

Citation:

Basit F and de Vries IJM (2019)
Dendritic Cells Require
PINK1-Mediated Phosphorylation of
BCKDE1 α to Promote Fatty Acid
Oxidation for Immune Function.
Front. Immunol. 10:2386.
doi: 10.3389/fimmu.2019.02386

Keywords: toll like 7/8 receptors, dendritic cell metabolism, branched chain amino acid (BCAA), PINK1, fatty acid oxidation (FAO)

INTRODUCTION

Dendritic cells (DCs) are specialized antigen presenting cells (APCs) in the immune system (1). DCs are central to pathogen sensing *via* an array of pathogen recognition receptors e.g., toll like receptors (TLRs) and stimulating antigen-specific T cells to proliferate and differentiate into effector and memory cells (2). Ligand binding to TLRs leads to DC activation and an enhanced capacity to stimulate T cells. DC activation is intrinsically linked to metabolic reprogramming (3). Currently, DC metabolism is mostly studied in the murine system, primarily using TLR4 agonist lipopolysaccharide (LPS) (4–7). Limited knowledge is available about the metabolic switch in human DCs (8–10). Furthermore, it is unclear whether all stimuli induce glycolysis in human DCs. In mice, TLR stimulation upregulates glycolysis, contributing to the metabolic requirements of high protein synthesis, a prerequisite for DC immune function. The TLR-stimulated “glycolytic burst” triggers *de novo* fatty acid synthesis through glucose-to-citrate metabolism, which is indispensable for DC function (4, 5).

Mitochondria are crucial for metabolic function. PTEN-induced putative kinase 1 (PINK1) predominantly localizes to the outer membrane of the mitochondria (11, 12) and is linked to mitochondrial function and subsequent metabolism (13). *PINK1* encodes a 581 amino acid protein with an N-terminal mitochondrial targeting sequence (MTS), a transmembrane domain (TMD), followed by a serine/threonine kinase domain. PINK1 is imported into mitochondria *via* the TOM or TIM23 complexes at the outer or inner mitochondrial membrane, respectively. Subsequently, its MTS is cleaved off by the mitochondrial processing peptidase located in the matrix. Afterwards, the inner mitochondrial membrane protease presenilin-associated rhomboid-like protease (PARL) cleaves PINK1 within the hydrophobic TMD between amino acids Ala103 and Phe104 (14–19). This generates 52 kDa N-terminally processed PINK1, which is released to the cytosol, where it is rapidly degraded by the proteasome through the N-end rule pathway (20). PINK1 is required for various cellular processes, e.g., regulation of mitochondrial bioenergetics through modulating complex I activity, promotion of mitophagy of depolarized mitochondria, protection against cell death, and protection of mitochondria via mitochondria-derived vesicles (MDV) (21).

Amino acids are the building blocks of proteins in mammals and their availability is of fundamental importance for cell survival, maintenance, and proliferation (22). Amino acids (23), especially glutamine (24–26), arginine (27, 28), and sulfur-containing amino acids (29) are of importance for the functioning of immune cells. Much less is known about the impact of branched-chain amino acids (BCAAs), valine, leucine, and isoleucine, on cells of the immune system. BCAA-transaminase converts BCAA into their corresponding branched-chain α -ketoacids (BCKAs). Then, BCKAs are catabolized by the branched-chain α -ketoacid dehydrogenase (BCKDH) complex within the mitochondrial matrix. Subsequently, acetyl-CoA is formed by metabolic reactions and incorporated into the tricarboxylic acid (TCA) cycle, or it enters the complex II of the electron transport chain (30). This process contributes to ATP production, which under physiological conditions is produced by OXPHOS. We here confirm previous results that a shift from OXPHOS to glycolysis occurs in human DCs stimulated with TLR4 agonist LPS (6). However, upon TLR7/8 stimulation of human DC we did not observe glycolysis. Instead we observed increased OXPHOS, which required FAO for immune function. These observations propose a scenario in which individual stimuli induce distinct metabolic reprogramming.

MATERIALS AND METHODS

Chemicals

Antimycin A (#A8674), Oligomycin A (#O4876), Rotenone (#R8875), Kinetin (#48130), Etomoxir (#E1905), Lipopolysaccharides from *Escherichia coli* 0111:B4 (#L4391), and 3,6-Dichloro-benzo[b]thiophene-2-carboxylic acid (#ENA018104907) were obtained from Sigma-Aldrich.

MitoTracker™ Green FM (#M7514), and 2-NBDG (#N13195) were obtained from Thermo Fisher Scientific.

Human DC Culture and Stimulation

Human monocyte-derived DCs were differentiated from peripheral blood monocytes as follows. Buffy coats were obtained from healthy volunteers (Sanquin, Nijmegen, Netherlands) according to institutional guidelines. Peripheral blood mononuclear cells (PBMCs) were isolated by using Ficoll density centrifugation (Lymphoprep; Axis-Shield PoC AS, Oslo, Norway). Monocytes were isolated from peripheral blood mononuclear cells (PBMC) by adherence, as described previously (31) and cultured in complete DC medium supplemented with human recombinant GM-CSF (20 ng/mL) plus human recombinant IL-4 (20 ng/mL) (PeproTech) for 7 days. To generate immunosuppressive DC, 10^{-6} M Dexamethasone was added at day 3 in culture. On day 6 or 7, DCs were harvested, stimulated with LPS or protamine-RNA (pRNA) complex, which was made freshly before being added to the cells. Protamine (protaminehydrochloride MPH 5000 IE/ml; Meda Pharma BV Amstelveen, Netherlands) was diluted to 0.5 mg/ml in RNase free water and mixed with 2 kbp-long single-stranded mRNA (coding for gp100). It was extensively mixed and incubated for 5–10 min at room temperature, before adding to the cells.

siRNA Transfection

For RNA interference, cells were transfected with SilencerSelect siRNA (Invitrogen), control siRNA (4390843), and siRNA targeting PINK1 (#s35166 and #s35168). At day 4 of the culture, the cells were harvested, washed with PBS, brought to a concentration of 1×10^6 cells/100 μ L resuspension buffer, and finally, transfected by electroporation with either 10 nM anti-PINK1 siRNA (#s35166) in combination with 10 nM anti-PINK1 siRNA (#s35168) or 20 nM control siRNA using the Neon transfection system (Invitrogen), according to the manufacturer's instructions. Electroporation was carried out with an electroporator (Neon with pipette station; Invitrogen) using three pulses (10 ms pulse width; 1350 V). After electroporation, cells were taken up in 10% FCS basal media without antibiotics and plated at 200 cells/ μ L. The next morning, the media was re-supplemented with penicillin, streptomycin, rGM-CSF, and rIL-4. At day 6, the cells were harvested, stimulated, and analyzed. Silencing efficiency was determined by western blot and qPCR of day 6 cells.

Cytokine Detection

Supernatant was taken from each sample after incubation and analyzed with standard sandwich ELISAs to detect TNF- α using human TNF- α ELISA Kit (#88-7346-22) from Thermo Fisher Scientific.

Flow Cytometry

Cell viability was determined using Fixable Viability Dye eFluor™ 780 (Invitrogen # 65-0865-14) according to manufacturer's instructions. Briefly, cells were incubated with Fixable Viability Dye eFluor™ 780 (1:2,000) at 4°C for 20 min. Subsequently, cells were washed and analyzed by flow

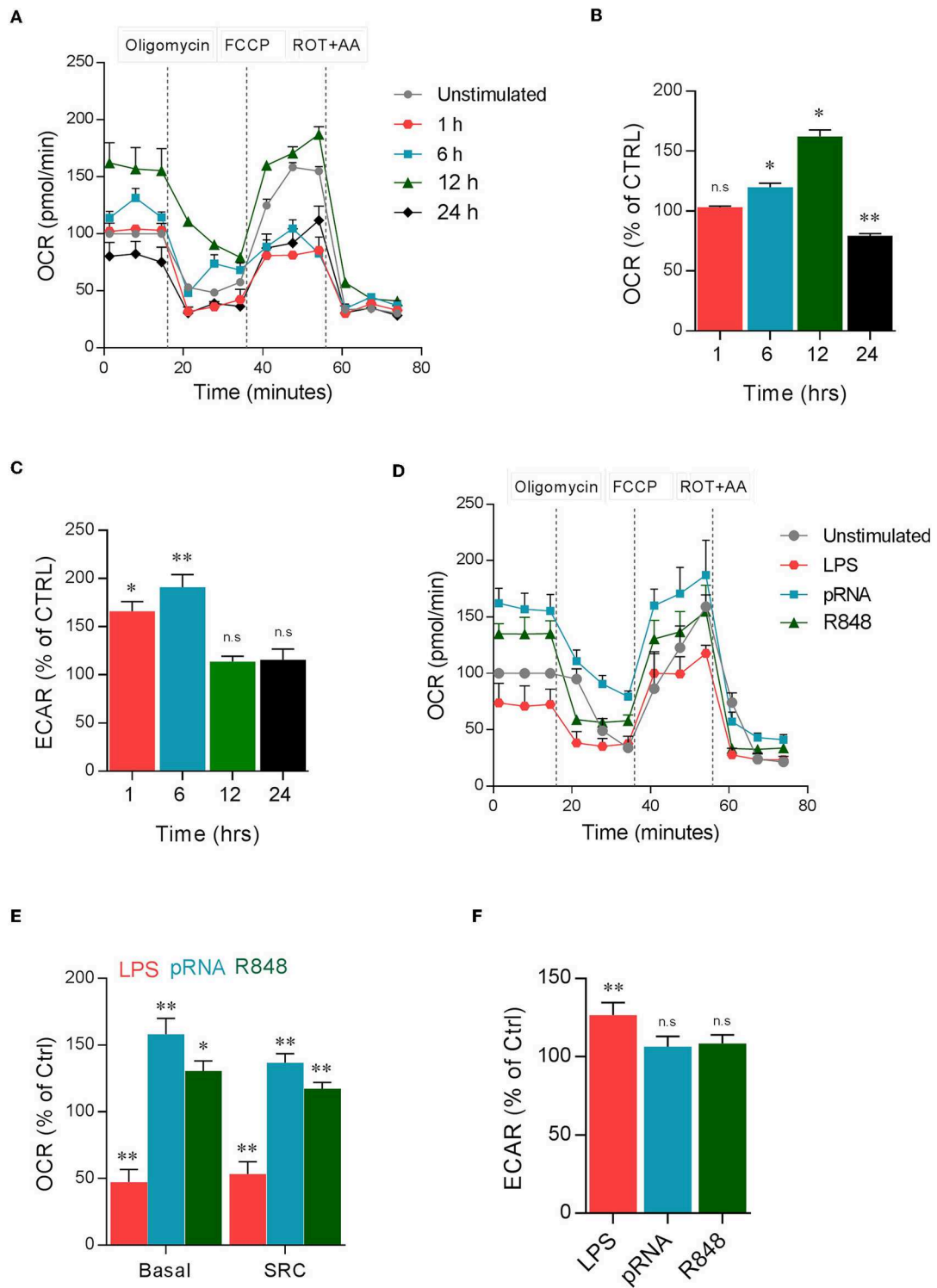


FIGURE 1 | TLR ligands induced metabolic changes in DC. **(A)** Mitochondrial fitness test of DCs stimulated with pRNA for indicated time points. Data represents mean ± SEM of three independent experiments. **(B,C)** Data was collected within same experiments as **(A)**, but is shown separately for better understanding. Data represents mean ± SEM of three independent experiments performed in triplicate. **p* < 0.05; ***p* < 0.01 (two-way ANOVA). **(D)** Mitochondrial fitness test of DCs stimulated with LPS (100 ng/mL), pRNA and R848 (1 μg/ml) for 12 h. Data represents mean ± SEM of three independent experiments performed in triplicate. **(E,F)** Data was collected within same experiments as **(D)**, but is shown separately for better understanding. Data represents mean ± SEM of three independent experiments performed in triplicate. **p* < 0.05; ***p* < 0.01 (two-way ANOVA).

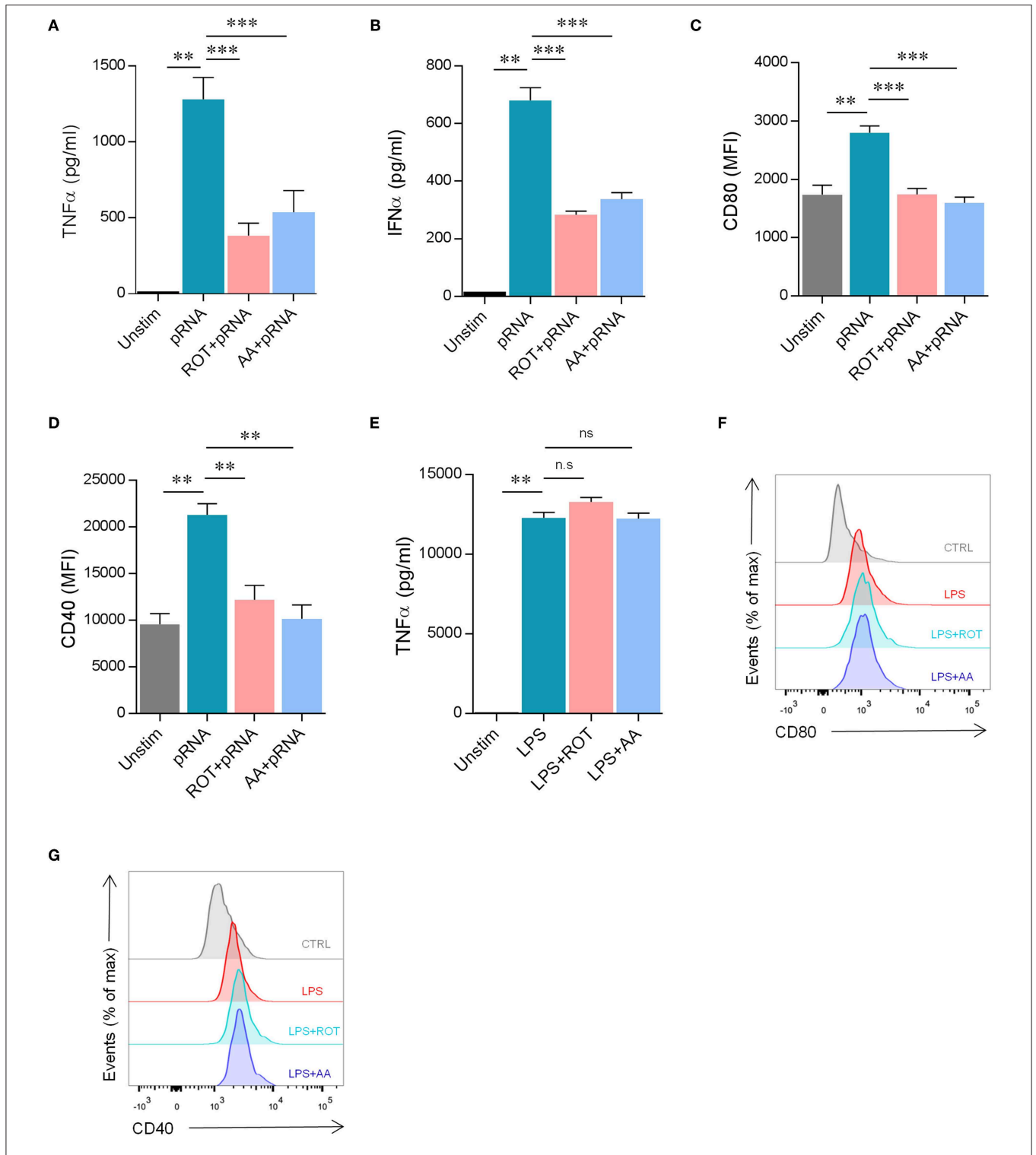


FIGURE 2 | pRNA stimulation-induced OXPPOS is required for DC maturation. **(A)** TNF α levels on protein level were measured in the supernatant of the DCs stimulated with pRNA for 12 h in the presence or absence of 10 nM rotenone or 10 nM antimycin A. Data represents mean \pm SEM of three independent experiments performed in triplicate. **(B)** IFN α levels on protein level were measured in the supernatant of the DCs stimulated for 12 h with pRNA in the presence or absence of 10 nM rotenone or 10 nM antimycin A. Data represents mean \pm SEM of three independent experiments performed in triplicate. **(C)** Mean fluorescence intensity of CD80 in DCs stimulated for 12 h with pRNA in the presence or absence of 10 nM rotenone or 10 nM antimycin A. Data represents mean \pm SEM of three independent experiments performed in triplicate. **(D)** Mean fluorescence intensity of CD40 in DCs stimulated for 12 h with pRNA in the presence or absence of 10 nM rotenone or 10 nM antimycin A. Data represents (Continued)

FIGURE 2 | mean \pm SEM of three independent experiments performed in triplicate. ** $p < 0.01$ (Student's *t*-test). **(E)** TNF α levels on protein level were measured in the supernatant of the DCs stimulated with LPS (100 ng/mL) for 12 h in the presence or absence of 10 nM rotenone or 10 nM antimycin A. Data represents mean \pm SEM of three independent experiments performed in triplicate. ** $p < 0.01$ (Student's *t*-test) **(F)** Expression of CD80 on DCs stimulated with LPS (100 ng/mL) for 12 h in the presence or absence of 10 nM rotenone or 10 nM antimycin A. One experiment of 3 is shown. **(G)** Expression of CD40 on DCs stimulated with LPS (100 ng/mL) for 12 h in the presence or absence of 10 nM rotenone or 10 nM antimycin A. One experiment of 3 is shown.

cytometry. The following primary monoclonal antibodies (mAbs) were used to determine the maturation state of the DCs: anti-CD80-APC, anti-CD40-APC (all BD Bioscience, San Jose, CA). Measurements were performed on FACSVerser flowcytometers (BD).

Metabolism Assays

An XF-96 Extracellular Flux Analyzer (Seahorse Bioscience) was used for Extracellular flux analyses of Dcscs (50,000 cells/well) (32). For mitochondrial fitness tests, OCR was measured sequentially at basal, and following the addition of 1 μ M oligomycin, 3 μ M FCCP (fluorocarbonyl cyanide phenylhydrazone), 1 μ M ROT+1 μ M AA. Fatty acid oxidation was determined by monitoring the OCR of cells by using a FAO inhibitor, etomoxir (40 μ M) in substrate limited medium. FAO was quantified as a response to etomoxir treatment as previously described (33, 34). For the glycolysis stress test, ECAR was measured sequentially at basal, and following the addition of 10 mM glucose, 1 μ M oligomycin and 50 mM 2-DG. Intracellular concentrations of Branched Chain Amino Acid (BCAA) were measured using colorimetric BCAA Assay Kit (#MET-5056, Cell Biolabs), as per manufacturer's instructions. Contribution of OXPHOS and glycolysis to ATP production was calculated as previously described (35).

Quantitative Real-Time PCR (qPCR)

qPCR was carried out in a 25- μ l reaction mixture containing 2 μ l of cDNA, 12.5 μ l of SYBR Green master mix (Applied Biosystems #A25742, Austin, USA), and 250 nmol of forward and reverse primer. The reaction conditions were as follows: 50°C for 2 min, 95°C for 10 min, and then 40 cycles of 95°C for 15 s and 60°C for 1 min. For qPCR, the primer sequences used are listed in **Supplementary Table 1**.

Cellular ATP Measurements

The levels of ATP were assessed using ATP Bioluminescence Assay Kit CLS II (#11699695001, Roche GmbH, Mannheim, Germany), according to the manufacturer's protocol.

Western Blot Antibodies and Detection

The PVDF membrane was probed with rabbit anti-PINK1 (#6946P; Cell Signaling), rabbit anti-Phospho (S293) BCKDE1A (#BET A304-672A-M; Bethyl Laboratories), anti-BCKDE1A (H-5) (#sc-271538; Santa Cruz Biotechnology) and mouse β -actin (#A5541; Sigma-Aldrich), followed by goat-anti-mouse or goat-anti-rabbit labeled with IRDye infrared dyes (LI-COR Biosciences, Leusden, Netherlands). A LI-COR Odyssey CLX infrared imaging system (LI-COR) was used for fluorescence detection.

Statistical Analysis

Comparisons for two groups were calculated using unpaired 2-tailed Student *t*-tests with Microsoft Excel. A 2-way ANOVA with a Bonferroni post-test was used for comparison of more than two groups using GraphPad Prism 6 software (GraphPad). Differences were considered significant at $P < 0.05$.

RESULTS

TLR Agonists Differentially Engage Metabolic Pathways in Human Dendritic Cells (DC)

To study metabolic adaptations, human DC were stimulated with TLR7/8 ligand pRNA in a time-dependent manner. pRNA stimulation of DC increased oxygen consumption rate (OCR) after 1, 6, and 12 h of stimulation but decreased OCR after 24 h of stimulation (**Figures 1A,B**). Analysis of extracellular acidification rate (ECAR) revealed that pRNA stimulation increased glycolysis after 1 and 6 h but not after 12 and 24 h of stimulation (**Figure 1C**). Given the maximum increase in OCR and absence of glycolysis at 12 h after pRNA stimulation, 12 h time point was chosen for further experiments. Next, DCs were stimulated with three different TLR ligands for 12 h. LPS (TLR4), R848 (TLR8), and pRNA (TLR7/8). LPS stimulation of DCs decreased basal OCR, spare respiratory capacity SRC (**Figures 1D,E**), and ATP-linked respiration (**Supplementary Figure 1A**). This indicates induction of glycolysis which was underscored by the increase of ECAR (**Figure 1F**) upon LPS stimulation. In contrast, pRNA and R848 stimulation of DCs increased basal OCR, SRC (**Figures 1D,E**), and ATP-linked respiration indicating upregulation of OXPHOS (**Supplementary Figure 1A**). pRNA and R848 stimulation did not increase glycolysis, as ECAR did not change (**Figure 1F**). Furthermore, no increase in 2-NBDG uptake was observed in pRNA-stimulated DC (**Supplementary Figure 1B**) also demonstrating the absence of glycolysis induction.

The absence of glycolysis induction and the upregulation of OXPHOS in pRNA-stimulated DCs led to the question of whether OXPHOS is required for proper maturation of DCs. Upon activation, immature DCs undergo maturation which is crucial for effective antigen presentation and initiation of the primary immune response. Maturation of DCs is characterized by the high expression of antigen-presenting and costimulatory molecules and the production of pro-inflammatory cytokines. Here, the secretion of pro-inflammatory cytokine TNF α and IFN α and membrane expression of costimulatory molecules CD40 and CD80 was assessed. Inhibiting OXPHOS by Rotenone (ROT) or Antimycin A (AA) significantly reduced both the secretion of TNF α and

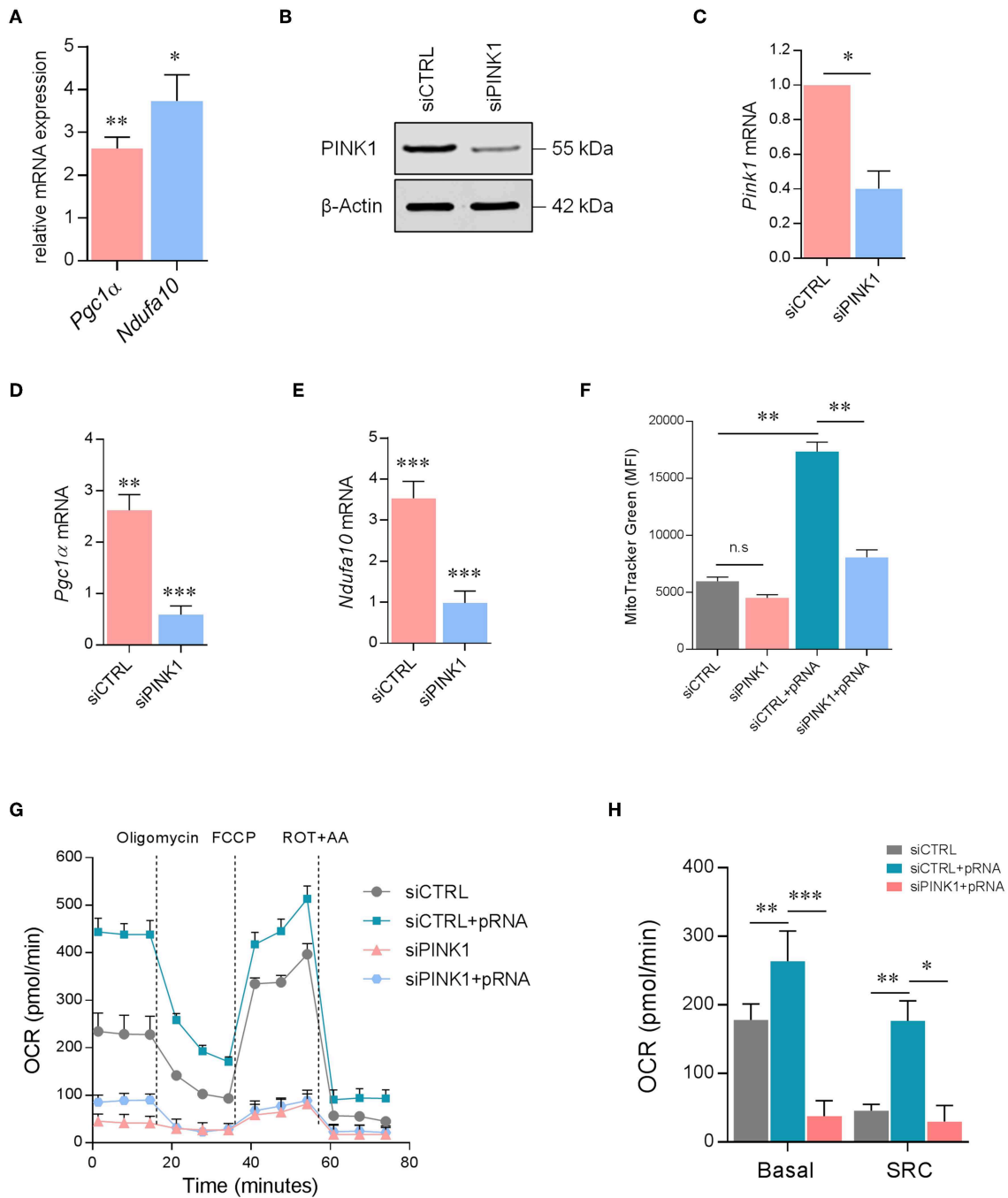


FIGURE 3 | PINK1 is required for OXPHOS in pRNA-stimulated DC. **(A)** Relative mRNA levels were analyzed after 12 h of pRNA stimulation by (qPCR) and normalized to β -actin expression by using the $2^{-\Delta\Delta CT}$ method. Data represents Mean \pm SEM of three independent experiments performed in triplicate. * $p < 0.05$; ** $p < 0.01$ (two-way ANOVA). **(B)** DCs transfected with a control siRNA (siCTRL) and pool of two PINK1-targeting siRNAs. Expression of PINK1 was determined by western blotting. β -actin was used as a loading control. **(C)** *PINK1* mRNA levels were analyzed by qPCR and normalized to β -actin expression by using the $2^{-\Delta\Delta CT}$ method. Data represents Mean \pm SEM of three independent experiments performed in triplicate. * $p < 0.05$ (Student's *t*-test). **(D,E)** mRNA levels were analyzed after 12 h of pRNA stimulation by (qPCR) and normalized to β -actin expression by using the $2^{-\Delta\Delta CT}$ method. Data represents Mean \pm SEM of three independent experiments performed in triplicate. ** $p < 0.01$; *** $p < 0.001$ (Student's *t*-test). **(F)** Mean fluorescence intensity of DCs stained with MitoTracker Green^{FM} after 12 h of pRNA stimulation. Data represents Mean \pm SEM of three independent experiments performed in triplicate. ** $p < 0.01$ (Student's *t*-test). **(G)** Mitochondrial fitness test of DCs stimulated with pRNA for 12 h. Data represents mean \pm SEM of three independent experiments performed in triplicate. **(H)** Data was collected within same experiments as **(G)**, but is shown separately for better understanding. Data represents mean \pm SEM of three independent experiments performed in triplicate. * $p < 0.05$; ** $p < 0.01$; *** $p < 0.001$ (Student's *t*-test).

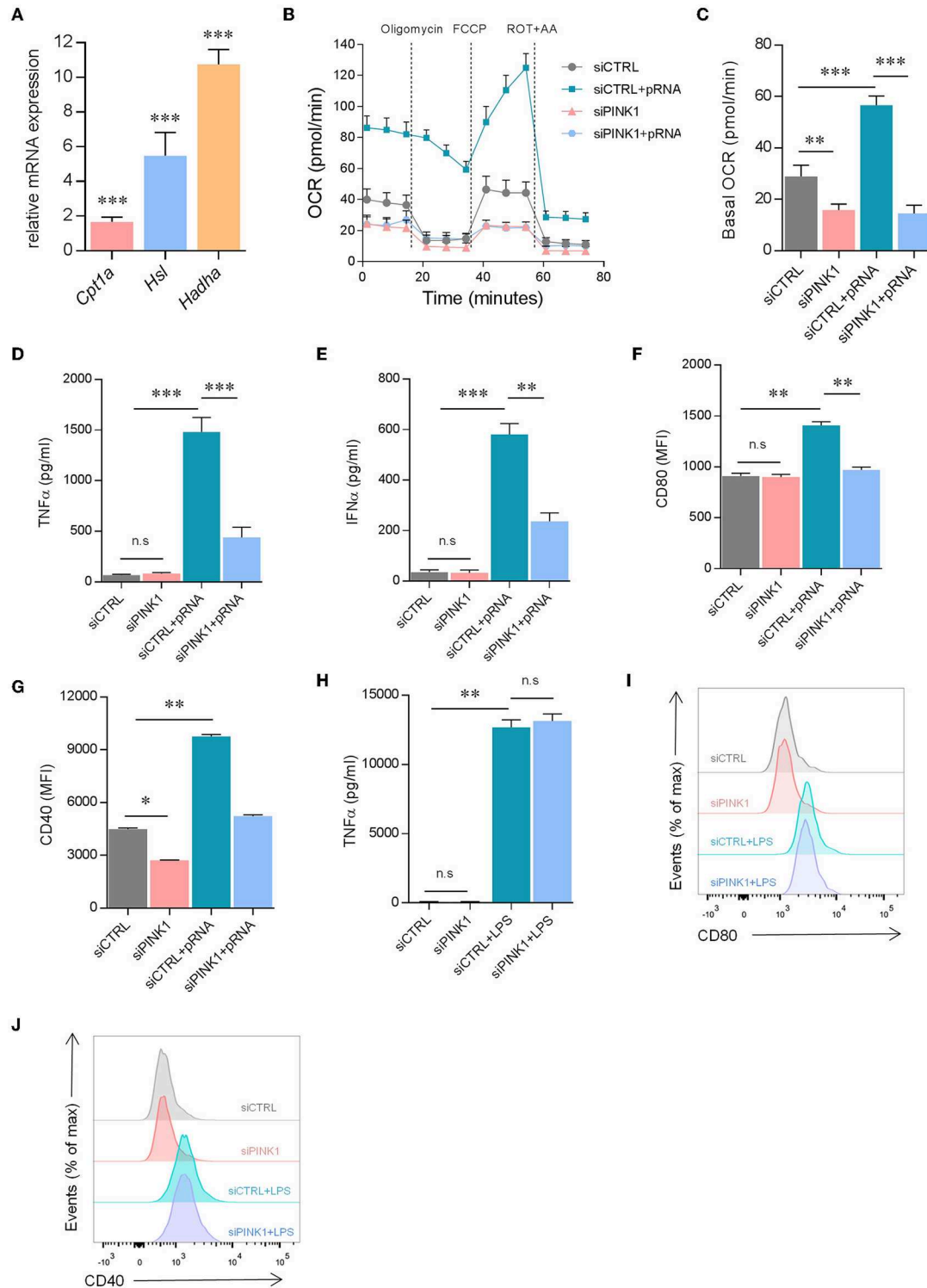


FIGURE 4 | pRNA-stimulated DC maturation requires PINK1-dependent FAO. **(A)** Relative mRNA levels were analyzed after 12 h of pRNA stimulation by (qPCR) and normalized to β-actin expression by using the $2^{-\Delta\Delta CT}$ method. Data represents Mean ± SEM of three independent experiments performed in triplicate. *** $p < 0.001$ (two-way ANOVA). **(B)** OCR was measured in DCs cultured in substrate-limited medium to indicate oxidation of endogenous fatty acids. Quantification of total FAO as the difference between conditions with or without Etomoxir treatment is shown. Data represents mean ± SEM of three independent experiments two-way ANOVA. (Continued)

FIGURE 4 | (C) Data was collected within same experiments as **(B)**, but is shown separately for better understanding. Data represents mean \pm SEM of three independent experiments two-way ANOVA. $**p < 0.01$; $***p < 0.001$ (Student's *t*-test). **(D)** TNF α levels on protein level were measured in the supernatant of the DCs stimulated with pRNA for 12 h. Data represents mean \pm SEM of three independent experiments performed in triplicate. $***p < 0.001$ (Student's *t*-test). **(E)** IFN α levels on protein level were measured in the supernatant of the DCs stimulated with pRNA for 12 h. Data represents mean \pm SEM of three independent experiments performed in triplicate. $**p < 0.01$; $***p < 0.001$ (Student's *t*-test). **(F)** Mean fluorescence intensity of CD80 in DCs stimulated for 12 h with pRNA. Data represents mean \pm SEM of three independent experiments performed in triplicate. $**p < 0.01$; $***p < 0.001$ (Student's *t*-test). **(G)** Mean fluorescence intensity of CD40 in DCs stimulated for 12 h with pRNA. Data represents mean \pm SEM of three independent experiments performed in triplicate. $*p < 0.05$; $**p < 0.01$; (Student's *t*-test). **(H)** TNF α levels on protein level were measured in the supernatant of the DCs stimulated with LPS (100 ng/mL) for 12 h. Data represents mean \pm SEM of three independent experiments performed in triplicate. $**p < 0.01$ (Student's *t*-test). **(I)** Expression of CD80 on DCs stimulated with LPS (100 ng/mL) for 12 h. One experiment of 3 is shown. **(J)** Expression of CD40 on DCs stimulated with LPS (100 ng/mL) for 12 h. One experiment of 3 is shown.

IFN α (**Figures 2A,B**) and the upregulation of CD40 and CD80 on pRNA-stimulated DC (**Figures 2C,D**). pRNA alone or in combination with ROT and AA did not affect cell viability (**Supplementary Figure 1C**). ROT or AA did not affect TNF α secretion (**Figure 2E**) and upregulation of CD40 and CD80 on LPS-stimulated DC (**Figures 2F,G**). Collectively, these data indicate pRNA-stimulated DC maturation requires OXPHOS but not glycolysis.

pRNA-Induced Dendritic Cell Maturation Requires Fatty Acid Oxidation (FAO)

To unravel the mechanism driving OXPHOS-mediated DC maturation after pRNA stimulation, *Ndufa10* and *Pgc1 α* gene expression was determined. Peroxisome proliferator-activated receptor gamma co-activator 1-alpha (PGC1 α) controls mitochondrial biogenesis (36–38). *Ndufa10* protein is a subunit of OXPHOS complex I (39). pRNA stimulation of DCs significantly increased *Pgc1 α* and *Ndufa10* expression, pointing to an increased mitochondrial biogenesis and OXPHOS activity (**Figure 3A**). Indeed, pRNA stimulation significantly increased mitochondrial content in DC (**Figure 3F**).

A critical regulator of OXPHOS and mitochondrial homeostasis is PINK1 (40–42). Effective silencing of PINK1 with siRNA (**Figures 3B,C**) significantly reduced *Pgc1 α* (**Figure 3D**) and *Ndufa10* in pRNA-stimulated DC (**Figure 3E**). As expected, based on the decrease of *Pgc1 α* , the mitochondrial content was lower in PINK1 deficient- compared to PINK1 proficient-DC (**Figure 3F**). Furthermore, the mitochondrial stress test showed that PINK1-silencing significantly reduced basal OCR, SRC (**Figures 3G,H**), and ATP-linked OCR (**Supplementary Figure 1D**) in both unstimulated- and pRNA-stimulated DC. Together, these findings indicate that PINK1 is required for pRNA-induced OXPHOS in DC maturation.

To determine how OXPHOS is increased in pRNA-stimulated DC we investigated the involvement of FAO. Previously, FAO-supplemented OXPHOS was shown in TLR9 stimulated plasmacytoid DCs (pDCs) (43). Here, we show that pRNA stimulation significantly increased expression of *Cpt1 α* , *Hadha* and *Hsl* in DC (**Figure 4A**). These genes encode enzymes for FAO regulation. A significant increase in FAO was observed in pRNA-stimulated DC (**Figures 4B,C**; **Supplementary Figure 1E**). PINK1 silencing reduced FAO in both unstimulated- and pRNA-stimulated DC

(**Figures 4B,C**; **Supplementary Figure 1E**). Collectively, these data indicate that FAO is involved in OXPHOS increase in pRNA-stimulated DC.

To investigate whether pRNA-stimulated DC maturation requires PINK1 regulated metabolic changes, the secretion of pro-inflammatory cytokine TNF α and IFN α and membrane expression of costimulatory molecules CD40 and CD80 were assessed. Upon pRNA stimulation, PINK1 knockdown DC were viable (cell viability over 97%, **Supplementary Figure 2A**) but produced significantly less TNF α and IFN α compared to PINK1 proficient cells (**Figures 4D,E**). Moreover, increased expression of CD40 and CD80 following pRNA stimulation was also significantly inhibited by PINK1 knockdown (**Figures 4F,G**). However, PINK1 knockdown did not affect LPS stimulated TNF α secretion (**Figure 4H**) or expression of CD80 and CD40 (**Figures 4I,J**). Together, this indicates that pRNA-mediated DC maturation is dependent on PINK1-regulated FAO.

PINK1-Mediated Phosphorylation of BCKDE1 α Is Required for pRNA-Induced Maturation of Dendritic Cells

pRNA-mediated TLR stimulation promotes FAO in DCs. *Pgc1 α* expression and FAO is increased by BCAA in myotubes (44). We hypothesize that TLR stimulation increases BCAA levels in DCs, leading to enhanced FAO. Indeed, pRNA stimulation significantly increased BCAA levels in DC (**Figure 5A**). The homeostasis of BCAA is critically regulated by branched-chain α -ketoacid dehydrogenase (BCKDH) complex, which oxidatively decarboxylates branch-chain α -ketoacids (BCKA) from BCAA. BCKDH is regulated by phosphorylation and dephosphorylation events. BCKDH kinase inactivates the complex by phosphorylation of the E1 α subunit of the complex, while BCKDH phosphatase activates the complex by dephosphorylation of E1 α . BCKDH kinase is crucial in the regulation of BCKDH activity (45). Modulation of BCKDH kinase activity changes BCAA homeostasis. 3,6-Dichloro-benzo[b]thiophene-2-carboxylic acid (BT2) is an inhibitor of BCKDH kinase (46). Here, inhibitor BT2 significantly reduced basal and pRNA stimulation-induced BCAA levels in DCs (**Figure 5A**), indicating involvement of BCKDH kinase. Importantly, BT2 significantly reduced pRNA-stimulated FAO in DC (**Figures 5B,C**; **Supplementary Figure 1F**).

We here show that PINK1-dependent FAO requires BCAA. PINK1 phosphorylates several proteins (11, 40, 47–50) and might therefore also regulate BCKDH. Indeed, pRNA stimulation

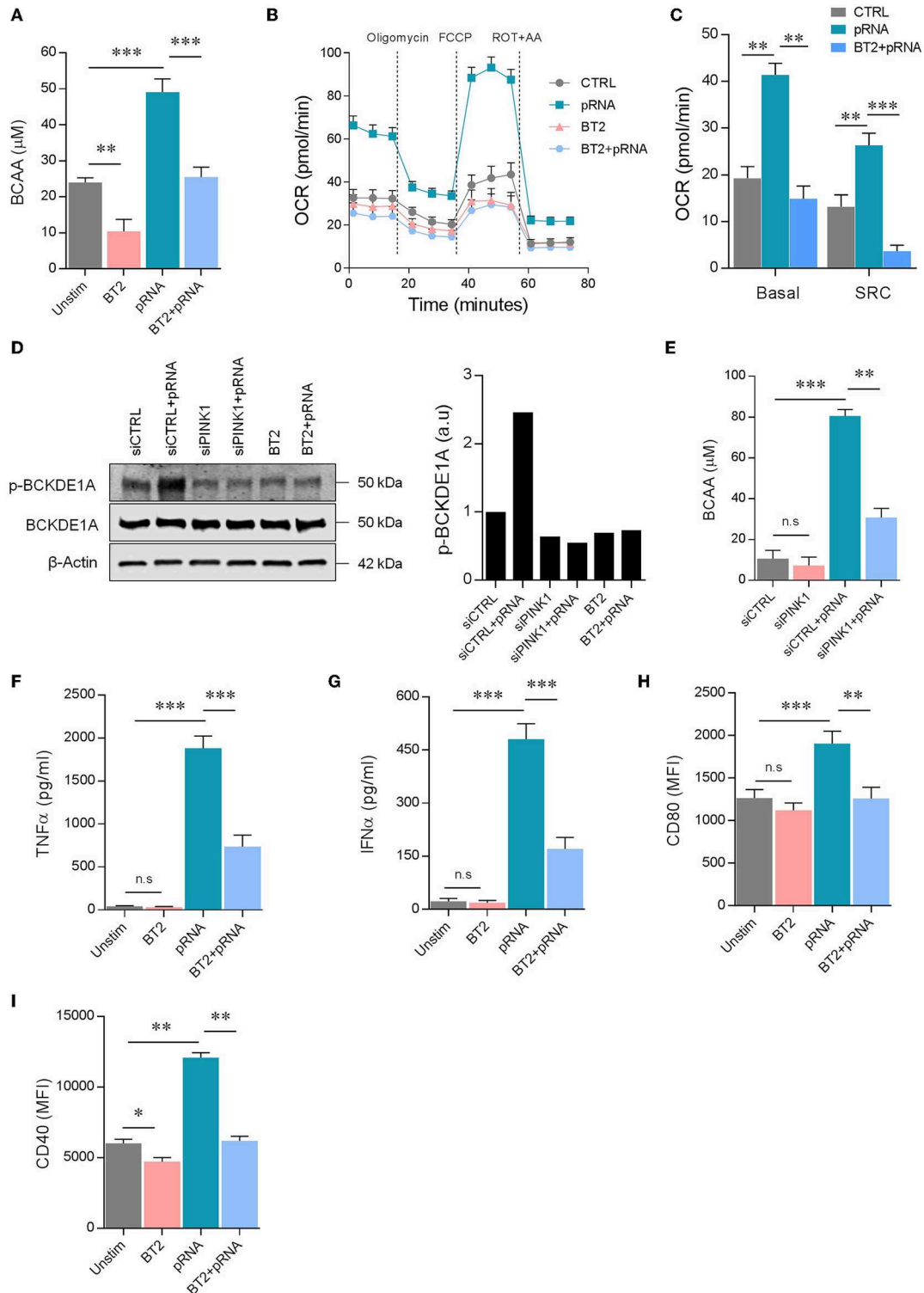


FIGURE 5 | PINK1 regulated BCAAs induce FAO in pRNA-stimulated DC. **(A)** Total BCAA concentrations were measured in the DCs stimulated for 12 h with pRNA in the presence or absence of 50 μM BT2, using a colorimetric assay kit. Data represents Mean \pm SEM of three independent experiments performed in triplicate. $**p < 0.01$; $***p < 0.001$ (Student's *t*-test). **(B)** OCR was measured in DC cultured in substrate-limited medium in the presence or absence of 50 μM BT2. Quantification of total FAO as the difference between conditions with or without Etomoxir treatment is shown. Data represents mean \pm SEM of three independent experiments performed in triplicate. **(C)** Data was collected within same experiments as **(B)**, but is shown separately for better understanding. Data represents mean \pm SEM of three independent experiments performed in triplicate. $**p < 0.01$; $***p < 0.001$ (Student's *t*-test). **(D)** Protein levels of phosphorylated p-BCKDE1 α and total BCKDE1 α (Continued)

FIGURE 5 | in DCs stimulated for 12 h with pRNA under indicated conditions. β -actin was used as a loading control. **(E)** Total BCAA concentrations were measured in siControl or siPINK1 transfected DCs using a colorimetric assay kit. Data represents Mean \pm SEM of three independent experiments performed in triplicate. $**p < 0.01$; $***p < 0.001$ (Student's *t*-test). **(F)** TNF α levels on protein level were measured in the supernatant of the DCs stimulated for 12 h with pRNA in the presence or absence of 50 μ M BT2. Data represents mean \pm SEM of three independent experiments performed in triplicate. $***p < 0.001$ (Student's *t*-test). **(G)** IFN α levels on protein level were measured in the supernatant of the DCs stimulated for 12 h with pRNA in the presence or absence of 50 μ M BT2. Data represents mean \pm SEM of three independent experiments performed in triplicate. $***p < 0.001$ (Student's *t*-test). **(H)** Mean fluorescence intensity of CD80 in DCs stimulated for 12 h with pRNA in the presence or absence of 50 μ M BT2. Data represents mean \pm SEM of three independent experiments performed in triplicate. $**p < 0.01$; $***p < 0.001$ (Student's *t*-test). **(I)** Mean fluorescence intensity of CD40 in DCs stimulated for 12 h with pRNA in the presence or absence of 50 μ M BT2. Data represents mean \pm SEM of three independent experiments performed in triplicate. $*p < 0.05$; $**p < 0.01$ (Student's *t*-test).

increased phosphorylation of BCKDH subunit BCKDE1 α in DCs, which could be inhibited by BCKDH kinase inhibitor BT2 (**Figure 5D**). Knockdown of PINK1 or addition of BT2 reduced phosphorylation of BCKDE1 α , and thereby the BCAA levels were diminished in DCs and no increase was observed after pRNA stimulation (**Figure 5D**). Knockdown of PINK1 or addition of BT2 reduced TNF α and IFN α production and expression of CD40 and CD80 by pRNA-stimulated DCs (**Figures 4D–G, 5E–I**). Collectively, these data show that DC maturation requires kinase activity of PINK1 for BCKDE1 α phosphorylation. Phosphorylation of BCKDE1 α disrupts BCAA catabolism and thereby promotes FAO, resulting in maturation of DC after pRNA stimulation.

PINK1 Kinase Activity Determines Immune Stimulatory Capacity of Human DC

Various factors can transform immune-stimulatory DCs into immune-suppressive DCs, characterized by low expression of co-stimulatory molecules and altered cytokine production (51). Here, we generated immunosuppressive DCs by adding dexamethasone during culture (Dexa-DC). Indeed, the expression of co-stimulatory molecules i.e., CD40 and CD80 and the production of TNF α was low in Dexa-DC and this could not be increased by pRNA stimulation (**Figures 6D,E; Supplementary Figure 1H**). Moreover, Dexa-DC had lower PINK1 expression (**Figure 6A**) and lower levels of BCAA compared to DCs (**Figure 6B**). Kinetin, a membrane permeable precursor of ATP analog N⁶ furfuryl ATP (KTP), increases kinase activity of PINK1 (52). Here, kinetin significantly increased BCAA levels and CD40 expression but not CD80 expression in Dexa-DCs (**Figures 6B,D,E**). pRNA in combination with kinetin significantly increased CD40 and CD80 expression and the production of TNF α in Dexa-DC (**Figures 6C–E**). Together, these data show that an increase in PINK1 kinase activity restored the immune-stimulatory capacity of immune-suppressive Dexa-DC.

DISCUSSION

Pathogen recognition by antigen presenting cells to initiate immune responses is a key process in host defense. For *in vitro* studies, TLR4 ligand LPS is most commonly used to mimic inflammatory responses. LPS promotes metabolic rewiring resembling the Warburg effect in both DCs and bone marrow-derived macrophages (BMDMs) (53, 54). While

knowledge concerning molecular pathways controlling metabolic routes in DC is accumulating (55), the specificity of metabolic adaptations after stimulation with different TLR ligands is not studied in detail. Here, we demonstrate that stimulation of DC via TLR7/8 engages a different metabolic pathway than DC stimulated *via* TLR4. We here confirm previous results concerning LPS stimulation of DC resulting in a switch to glycolysis for maturation. In contrast, TLR7/8 stimulated DC increase OXPHOS concurrently with glycolysis. However, this glycolysis diminishes after 12 h while increased OXPHOS is maintained. A recent study demonstrated that different DC subtypes, i.e., human pDCs and monocyte-derived DCs (moDCs), have distinct metabolic requirements for maturation. Upon stimulation of RIG-I, moDC increase glycolysis whereas pDCs employ OXPHOS (56). Previously, we reported that human blood-derived DCs i.e., cDC2⁺ mDC and pDC for maturation switch to glycolysis and OXPHOS, respectively (25). This underlines the distinct metabolic adaptations triggered by different pathogens depending on their specific TLR binding.

Specific stimulation of DC via TLR7/8 by pRNA increased OXPHOS accompanied by an increased mitochondrial content. A critical regulator of OXPHOS and mitochondrial homeostasis is PINK1. Indeed, PINK1 knockdown reduced the pRNA-induced increase of OXPHOS and mitochondrial content. PINK1 is also involved in mitophagy and has a role in MHC antigen presentation (57–59). Lack of accumulation of mitochondrial content in PINK1 deficient cells upon pRNA stimulation indicates absence of mitophagy in our model (60). Albeit, our data show that PINK1 is crucial for pRNA-stimulated DC maturation, indicating a mitophagy-independent function of PINK1. Previously, PINK1 is described to be crucial for survival (61, 62). However, the viability of PINK1 knockdown DC was not affected either in the presence nor absence of pRNA (**Supplementary Information**). Furthermore, it is shown that PINK1 deficiency results in less ATP due to impaired mitochondrial fission leading to defective assembly of the ETC complexes, and reduction in mitochondrial respiration and mitochondrial buffering capacity (63–66). Total intracellular ATP levels were increased in both pRNA maturation of DC and PINK1-knockdown DC (**Supplementary Information**). We here show that PINK1 knockdown DC maintain cell viability by reprogramming bioenergetics from OXPHOS to glycolysis (**Supplementary Information**). Loss of PINK1 has been reported to result in stabilization of HIF1 α which stimulates glycolysis (67). Indeed, glucose uptake was increased in PINK1-deficient cells and further increased by pRNA

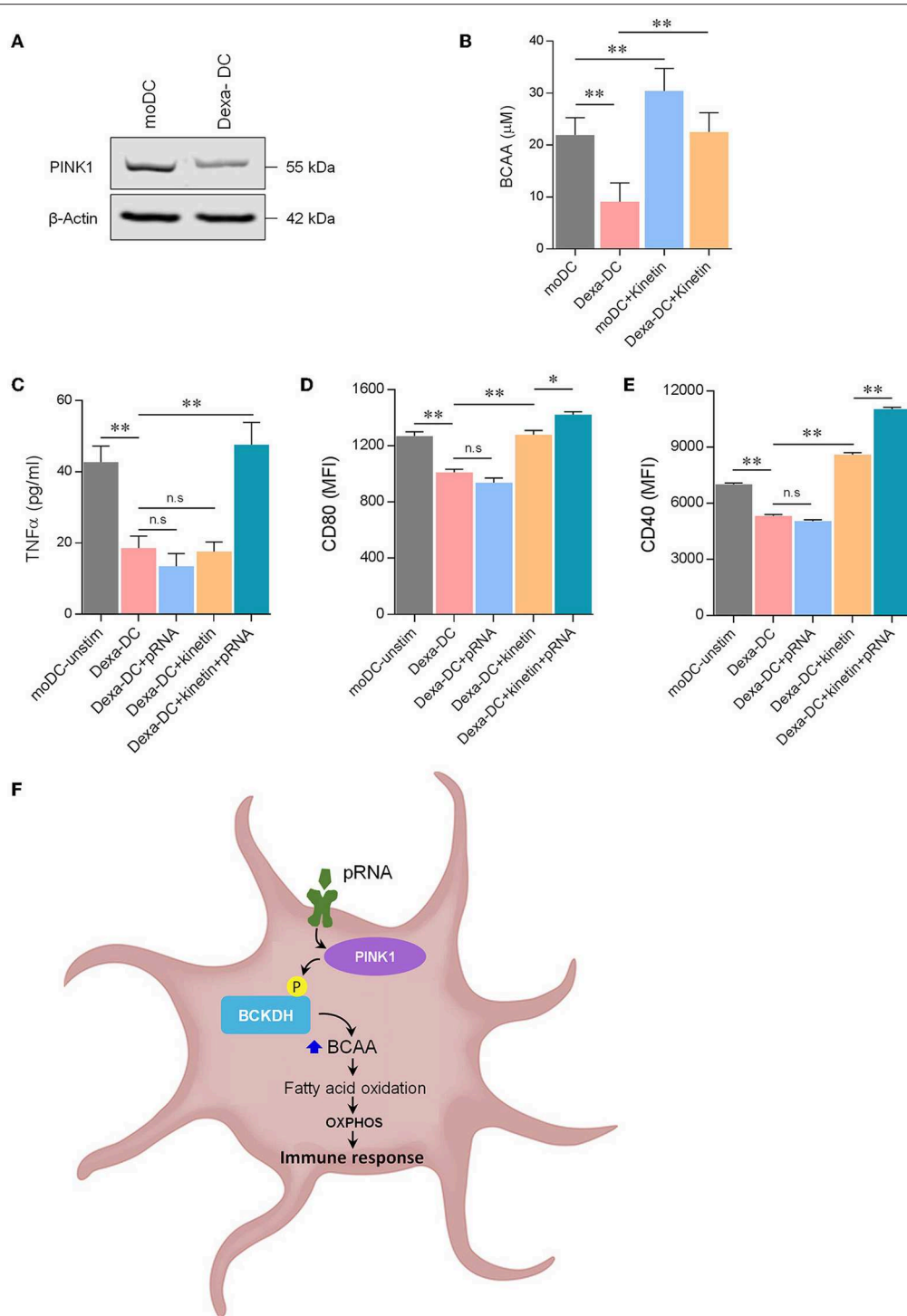


FIGURE 6 | Kinetin primes immunosuppressive DC for maturation. **(A)** Expression of PINK1 in DCs was determined by western blotting. β -actin was used as a loading control. **(B)** Total BCAA concentrations were measured in DCs, stimulated for 12 h with pRNA in the presence or absence of 20 μ M kinetin, using a colorimetric assay kit. Data represents Mean \pm SEM of three independent experiments performed in triplicate. $**p < 0.01$ (Student's *t*-test). **(C)** TNF α levels on protein level were measured in the supernatant of the DCs stimulated for 12 h with pRNA in the presence or absence of 20 μ M kinetin. Data represents mean \pm SEM of three independent experiments performed in triplicate. $**p < 0.01$ (Student's *t*-test). **(D)** Mean fluorescence intensity of CD80 in DCs stimulated for 12 h with pRNA in the presence or absence of 20 μ M kinetin. Data represents mean \pm SEM of three independent experiments performed in triplicate. $*p < 0.05$; $**p < 0.01$ (Student's *t*-test). **(E)** Mean fluorescence intensity of CD40 in DCs stimulated for 12 h with pRNA in the presence or absence of 20 μ M kinetin. Data represents mean \pm SEM of three independent experiments performed in triplicate. $**p < 0.01$ (Student's *t*-test). **(F)** Mechanistic model of OXPHOS-mediated DC activation. Activation of TLR7/8 with pRNA lead to increase in OXPHOS. pRNA stimulation phosphorylates BCKDE1 α in a PINK1-dependent manner. pRNA stimulation increased branched-chain amino acid (BCAA) to promote FAO. Increased FAO and OXPHOS were required for DC activation.

stimulation (**Supplementary Information**). Intriguingly, *Glut1* levels did not change upon pRNA stimulation, however loss of PINK1 increased *Glut1* levels, which has been reported to be involved in glucose uptake in DCs (68). These data suggest that loss of PINK1 reprograms glucose metabolism (**Supplementary Information**), possibly through HIF1 α , in DCs to sustain cell viability.

We here identified PINK1 as a novel regulator of BCAAs, which are important for FAO to supplement OXPHOS crucial for TLR7/8-induced DC maturation. The activity of BCKDH complex is regulated *via* phosphorylation/dephosphorylation of BCKDE1 α . Previously, PINK1 is shown to be able to phosphorylate target proteins in a kinase-dependent manner (11, 40, 47–50, 69). Our data show that PINK1 regulates phosphorylation of BCKDE1 α in DCs and thus is a critical regulator of BCKDH complex for BCAA catabolism. Interestingly, Parkinson disease patients, who have mutated PINK1 in neurons (64), have decreased BCAA serum levels associated with an increase in the clinical severity of the disease (70). Therefore, our finding that PINK1 regulates BCAA catabolism may have important implications for patients suffering from Parkinson disease. TLR7/8 stimulation with pRNA increased BCAA promoting FAO in DC. Similarly, for pDC maturation, TLR9 agonist, CpG-A, also enhanced FAO (43). In contrast, FAO is not necessary for maturation of mouse bone marrow-derived DCs stimulated with LPS (7). Collectively, DCs engage distinct metabolic routes for maturation upon stimulation *via* different TLRs.

Our data identified PINK1 as a critical regulator of BCAA catabolism, whereas previously PINK1 is shown to critically regulate FAO (71). This led to the question of whether PINK1 *via* BCAAs contribute to FAO. We observed that PINK1 knockdown reduced pRNA-induced FAO in DCs. BCAAs are required for fatty acid synthesis (72) and promote FAO in muscles and myotubes (44, 73). Consistently, inhibition of BCAAs levels abrogated pRNA-induced FAO in DC. BCAA leucine increases expression of *Cpt1*, *Cpt2* (74), *PPAR γ* (75), *Pgc1 α* , and *Nrf-1* (76). Indeed, *Pgc1 α* expression and mitochondrial content were increased after pRNA stimulation of DC, hinting at increased FAO. Another possible mechanism for BCAA-mediated FAO is that leucine increases SIRT1 activity, which in turn phosphorylates AMPK (76). AMPK subsequently regulates FAO through phosphorylation of acetyl-CoA carboxylase 2 (77). Given the increase in BCAA after TLR7/8 stimulation of DC by pRNA it seems likely that SIRT1-phospho AMPK increases FAO. An alternative mechanism for BCAA-mediated FAO could be that leucine inhibits mTOR (78), which is central to lipid homeostasis and mTOR inhibition increases FAO (79). Therefore, it is possible that pRNA stimulation of DC increased BCAA and thereby inhibited mTOR resulting in FAO.

In immunosuppressive DC (Dexa-DC), PINK1 levels were diminished and increasing PINK1 kinase activity directed the immunosuppressive phenotype toward an immunostimulatory

phenotype. Previously, Ibrahim et al. showed that DC with lower lipid content are immunosuppressive (80). PINK1 expression is indeed necessary for regulating lipid droplet formation and mitochondrial FAO (81). Activation of DC induces fatty acid synthesis, which results in increased lipid storage in lipid droplets (82). Together, these reports suggest that lower PINK1 levels likely result in reduced fatty acid synthesis and lipid storage in immunosuppressive DC. Induction of PINK1 kinase activity likely increased fatty acid synthesis *via* BCAAs in immunosuppressive DC, which was then utilized for FAO upon TLR7/8 stimulation. The observation that PINK1 levels were lower in immunosuppressive DC is in contrast with the observed effects in Parkinson patients and *Pink1*^{-/-} mice. There, high levels of TNF- α , IFN- γ , and IL-6 are all indicative of an inflammatory phenotype that are observed (83, 84). This can be due to reduced OXPHOS activity, mitophagy induction, and higher oxidized mtDNA, acting as an inflammatory signal in the Parkinson model (84, 85). Here, we observed an increase in OXPHOS activity and did not observe mitophagy possibly explaining the immune suppressive phenotype.

Our data, together with recent reports, show that distinct metabolic programs in DCs can be induced dependent on the stimulus. Manipulation of human DC functionality via metabolic programming needs a broader understanding, especially since the diversity of responses induced by different PRRs is very broad. We identified the PINK1-BCAAs axis as a novel metabolic programming pathway in DCs (**Figure 6F**), hence, strategies aiming at modifying this axis might provide a clinical benefit in immune-related pathologies.

DATA AVAILABILITY STATEMENT

All datasets generated for this study are included in the manuscript/**Supplementary Files**.

AUTHOR CONTRIBUTIONS

FB and IV conceived the research and wrote the manuscript. FB performed the experiments and analyzed the data. IV supervised the research.

FUNDING

This work was supported by NWO-grant 918.14.655 from the Netherlands Organization for Scientific Research and a PPP Allowance made available by Top Sector Life Sciences and Health (LSHGM18056-SGF).

SUPPLEMENTARY MATERIAL

The Supplementary Material for this article can be found online at: <https://www.frontiersin.org/articles/10.3389/fimmu.2019.02386/full#supplementary-material>

REFERENCES

- Tel J, Anguille S, Waterborg CE, Smits EL, Figdor CG, de Vries IJ. Tumoricidal activity of human dendritic cells. *Trends Immunol.* (2014) 35:38–46. doi: 10.1016/j.it.2013.10.007
- Hemmi H, Akira S. TLR signalling and the function of dendritic cells. *Chem Immunol Allergy.* (2005) 86:120–35. doi: 10.1159/000086657
- Mishra A. Metabolic plasticity in dendritic cell responses: implications in allergic asthma. *J Immunol Res.* (2017) 2017:5134760. doi: 10.1155/2017/5134760
- Amiel E, Everts B, Fritz D, Beauchamp S, Ge B, Pearce E, et al. Mechanistic target of rapamycin inhibition extends cellular lifespan in dendritic cells by preserving mitochondrial function. *J Immunol.* (2014) 193:2821–30. doi: 10.4049/jimmunol.1302498
- Krawczyk CM, Holowka T, Sun J, Blagih J, Amiel E, DeBerardinis R, et al. Toll-like receptor-induced changes in glycolytic metabolism regulate dendritic cell activation. *Blood.* (2010) 115:4742–9. doi: 10.1182/blood-2009-10-249540
- Thwe PM, Pelgrom L, Cooper R, Beauchamp S, Reisz JA, D'Alessandro A, et al. Cell-intrinsic glycogen metabolism supports early glycolytic reprogramming required for dendritic cell immune responses. *Cell Metab.* (2017) 26:558–67.e5. doi: 10.1016/j.cmet.2017.08.012
- Everts B, Amiel E, Huang SC, Smith AM, Lam WY, et al. TLR-driven early glycolytic reprogramming via the kinases TBK1-IKKvarepsilon supports the anabolic demands of dendritic cell activation. *Nat Immunol.* (2014) 15:323–32. doi: 10.1038/ni.2833
- Bajwa G, DeBerardinis RJ, Shao B, Hall B, Farrar J, Gill MA. Cutting edge: critical role of glycolysis in human plasmacytoid dendritic cell antiviral responses. *J Immunol.* (2016) 196:2004–9. doi: 10.4049/jimmunol.1501557
- Szatmari I, Torocsik D, Agostini M, Nagy T, Gurnell M, Barta E, et al. PPARgamma regulates the function of human dendritic cells primarily by altering lipid metabolism. *Blood.* (2007) 110:3271–80. doi: 10.1182/blood-2007-06-096222
- Ferreira GB, Vanherwegen AS, Eelen G, Gutierrez AC, Van Lommel L, Marchal K, et al. Vitamin D3 induces tolerance in human dendritic cells by activation of intracellular metabolic pathways. *Cell Rep.* (2015) 10:711–25. doi: 10.1016/j.celrep.2015.01.013
- Weihofen A, Thomas KJ, Ostaszewski BL, Cookson M, Selkoe DJ. Pink1 forms a multiprotein complex with Miro and Milton, linking Pink1 function to mitochondrial trafficking. *Biochemistry.* (2009) 48:2045–52. doi: 10.1021/bi8019178
- Zhou C, Huang Y, Shao Y, May J, Prou D, Perier C, et al. The kinase domain of mitochondrial PINK1 faces the cytoplasm. *Proc Natl Acad Sci USA.* (2008) 105:12022–7. doi: 10.1073/pnas.0802814105
- Voigt A, Berlemann LA, Winklhofer KF. The mitochondrial kinase PINK1: functions beyond mitophagy. *J Neurochem.* (2016) 139(Suppl 1):232–9. doi: 10.1111/jnc.13655
- Whitworth AJ, Lee JR, Ho VM, Flick R, Chowdhury R, McQuibban GA. Rhomboid-7 and HtrA2/Omi act in a common pathway with the Parkinsons disease factors Pink1 and Parkin. *Dis Model Mech.* (2008) 1:168–74. doi: 10.1242/dmm.000109
- Jin SM, Lazarou M, Wang C, Kane LA, Narendra D, Youle RJ. Mitochondrial membrane potential regulates PINK1 import and proteolytic destabilization by PARL. *J Cell Biol.* (2010) 191:933–42. doi: 10.1083/jcb.201008084
- Deas E, Plun-Favreau H, Gandhi S, Desmond H, Kjaer S, Loh S, et al. PINK1 cleavage at position A103 by the mitochondrial protease PARL. *Hum Mol Genet.* (2011) 20:867–79. doi: 10.1093/hmg/ddq526
- Meissner C, Lorenz H, Weihofen A, Selkoe DJ, Lemberg M, et al. The mitochondrial intramembrane protease PARL cleaves human Pink1 to regulate Pink1 trafficking. *J Neurochem.* (2011) 117:856–67. doi: 10.1111/j.1471-4159.2011.07253.x
- Shi G, Lee JR, Grimes DA, Racacho L, Ye D, Yang H, et al. Functional alteration of PARL contributes to mitochondrial dysregulation in Parkinsons disease. *Hum Mol Genet.* (2011) 20:1966–74. doi: 10.1093/hmg/ddr077
- Greene AW, Grenier K, Aguilera MA, Muise S, Farazifard R, Haque ME, et al. Mitochondrial processing peptidase regulates PINK1 processing, import and Parkin recruitment. *EMBO Rep.* (2012) 13:378–385. doi: 10.1038/embor.2012.14
- Yamano K, Youle RJ. PINK1 is degraded through the N-end rule pathway. *Autophagy.* (2013) 9:1758–69. doi: 10.4161/auto.24633
- McLelland GL, Soubannier V, Chen CX, McBride HM, Fon EA. Parkin and PINK1 function in a vesicular trafficking pathway regulating mitochondrial quality control. *EMBO J.* (2014) 33:282–95. doi: 10.1002/embj.201385902
- Grohmann U, Mondanelli G, Belladonna ML, Orabona C, Pallotta M, Iacono A, et al. Amino-acid sensing and degrading pathways in immune regulation. *Cytokine Growth Factor Rev.* (2017) 35:37–45. doi: 10.1016/j.cytogfr.2017.05.004
- Li P, Yin YL, Li D, Kim SW, Wu G. Amino acids and immune function. *Br J Nutr.* (2007) 98:237–252. doi: 10.1017/S000711450769936X
- Johnson MO, Wolf MM, Madden MZ, Andrejeva G, Sugiura A, Contreras DC, et al. Distinct regulation of Th17 and Th1 cell differentiation by glutaminase-dependent metabolism. *Cell.* (2018) 175:1780–95.e19. doi: 10.1016/j.cell.2018.10.001
- Basit F, Mathan T, Sancho D, de Vries IJM. Human dendritic cell subsets undergo distinct metabolic reprogramming for immune response. *Front Immunol.* (2018) 9:2489. doi: 10.3389/fimmu.2018.02489
- Cruzat V, Macedo Rogero M, Noel Keane K, Curi R, Newsholme P. Glutamine: metabolism and immune function, supplementation and clinical translation. *Nutrients.* (2018) 10:E1564. doi: 10.20944/preprints201809.0459.v1
- Kim SH, Roszik J, Grimm EA, Ekmekcioglu S. Impact of l-arginine metabolism on immune response and anticancer immunotherapy. *Front Oncol.* (2018) 8:67. doi: 10.3389/fonc.2018.00067
- Popovic PJ, Zeh HJ 3rd, Ochoa JB. Arginine and immunity. *J Nutr.* (2007) 137:1681S–6S. doi: 10.1093/jn/137.6.1681S
- Grimble RF. The effects of sulfur amino acid intake on immune function in humans. *J Nutr.* (2006) 136:1660S–5S. doi: 10.1093/jn/136.6.1660S
- Lerin C, Goldfine AB, Boes T, Liu M, Kasif S, Dreyfuss JM, et al. Defects in muscle branched-chain amino acid oxidation contribute to impaired lipid metabolism. *Mol Metab.* (2016) 5:926–36. doi: 10.1016/j.molmet.2016.08.001
- de Vries IJ, Eggert AA, Scharenborg NM, Vissers J, Lesterhuis WJ, et al. Phenotypic and functional characterization of clinical grade dendritic cells. *J Immunother.* (2002) 25:429–38. doi: 10.1097/00002371-200209000-00007
- Pelgrom LR, van der Ham AJ, Everts B. Analysis of TLR-induced metabolic changes in dendritic cells using the seahorse XF(e)96 extracellular flux analyzer. *Methods Mol Biol.* (2016) 1390:273–85. doi: 10.1007/978-1-4939-3335-8_17
- Pike LS, Smift AL, Croteau NJ, Ferrick D, Wu M. Inhibition of fatty acid oxidation by etomoxir impairs NADPH production and increases reactive oxygen species resulting in ATP depletion and cell death in human glioblastoma cells. *Biochim Biophys Acta.* (2011) 1807:726–34. doi: 10.1016/j.bbabo.2010.10.022
- Tu LN, Zhao AH, Hussein M, Stocco DM, Selvaraj V. Translocator protein (TSPO) affects mitochondrial fatty acid oxidation in steroidogenic cells. *Endocrinology.* (2016) 157:1110–21. doi: 10.1210/en.2015-1795
- Yang M, Chadwick AE, Dart C, Kamishima T, Quayle J. Bioenergetic profile of human coronary artery smooth muscle cells and effect of metabolic intervention. *PLoS ONE.* (2017) 12:e0177951. doi: 10.1371/journal.pone.0177951
- Austin S, St-Pierre J. PGC1alpha and mitochondrial metabolism—emerging concepts and relevance in ageing and neurodegenerative disorders. *J Cell Sci.* (2012) 125:4963–71. doi: 10.1242/jcs.113662
- Ugucioni G, Hood DA. The importance of PGC-1alpha in contractile activity-induced mitochondrial adaptations. *Am J Physiol Endocrinol Metab.* (2011) 300:E361–71. doi: 10.1152/ajpendo.00292.2010
- Fernandez-Marcos PJ, Auwerx J. Regulation of PGC-1alpha, a nodal regulator of mitochondrial biogenesis. *Am J Clin Nutr.* (2011) 93:884S–90. doi: 10.3945/ajcn.110.001917
- Hoefs SJ, van Spronsen FJ, Lenssen EW, Nijtmans LG, Rodenburg RJ, Smeitink JA, et al. NDUFA10 mutations cause complex I deficiency in a patient with Leigh disease. (2011) *Eur J Hum Genet.* 19:270–4. doi: 10.1038/ejhg.2010.204
- Morais VA, Haddad D, Craessaerts K, De Bock PJ, Swerts J, Vilain S, et al. PINK1 loss-of-function mutations affect mitochondrial complex I activity via Ndufa10 ubiquitination uncoupling. *Science.* (2014) 344:203–7. doi: 10.1126/science.1249161

41. Bueno M, Lai YC, Romero Y, Brands J, St. Croix C, Kamga C, et al. PINK1 deficiency impairs mitochondrial homeostasis and promotes lung fibrosis. *J Clin Invest.* (2015) 125:521–38. doi: 10.1172/JCI74942
42. Heeman B, Van den Haute C, Aelvoet SA, Valsecchi F, Rodenburg RJ, Reumers V, et al. Depletion of PINK1 affects mitochondrial metabolism, calcium homeostasis and energy maintenance. *J Cell Sci.* (2011) 124:1115–25. doi: 10.1242/jcs.078303
43. Wu D, Sanin DE, Everts B, Chen Q, Qiu J, Buck MD, et al. Type 1 interferons induce changes in core metabolism that are critical for immune function. *Immunity.* (2016) 44:1325–36. doi: 10.1016/j.immuni.2016.06.006
44. Liang C, Curry BJ, Brown PL, Zemel M. Leucine modulates mitochondrial biogenesis and SIRT1-AMPK signaling in C2C12 myotubes. *J Nutr Metab.* (2014) 2014:239750. doi: 10.1155/2014/239750
45. Wynn RM, Kato M, Machiusi M, Chuang JL, Li J, Tomchick DR, et al. Molecular mechanism for regulation of the human mitochondrial branched-chain alpha-ketoacid dehydrogenase complex by phosphorylation. *Structure.* (2004) 12:2185–96. doi: 10.1016/j.str.2004.09.013
46. Tso SC, Gui WJ, Wu CY, Chuang JL, Qi X, Skvora KJ, et al. Benzothioephene carboxylate derivatives as novel allosteric inhibitors of branched-chain alpha-ketoacid dehydrogenase kinase. *J Biol Chem.* (2014) 289:20583–93. doi: 10.1074/jbc.M114.569251
47. Pridgeon JW, Olzmann JA, Chin LS, Li L. PINK1 protects against oxidative stress by phosphorylating mitochondrial chaperone TRAP1. *PLoS Biol.* (2007) 5:e172. doi: 10.1371/journal.pbio.0050172
48. Plun-Favreau H, Klupsch K, Moiso N, Gandhi S, Kjaer S, Frith D, et al. The mitochondrial protease Htra2 is regulated by Parkinsons disease-associated kinase PINK1. *Nat Cell Biol.* (2007) 9:1243–52. doi: 10.1038/ncb1644
49. Chen Y, Dorn GW 2nd. PINK1-phosphorylated mitofusin 2 is a Parkin receptor for culling damaged mitochondria. *Science.* (2013) 340:471–5. doi: 10.1126/science.1231031
50. Arena G, Gelmetti V, Torosantucci L, Vignone D, Lamorte G, De Rosa P, et al. PINK1 protects against cell death induced by mitochondrial depolarization, by phosphorylating Bcl-XL and impairing its pro-apoptotic cleavage. *Cell Death Differ.* (2013) 20:920–30. doi: 10.1038/cdd.2013.19
51. Domogalla MP, Rostan PV, Raker VK, Steinbrink K. Tolerance through education: how tolerogenic dendritic cells shape immunity. *Front Immunol.* (2017) 8:1764. doi: 10.3389/fimmu.2017.01764
52. Hertz NT, Berthet A, Sos ML, Thorn KS, Burlingame AL, Nakamura K, et al. A neo-substrate that amplifies catalytic activity of parkinsons-disease-related kinase PINK1. *Cell.* (2013) 154:737–47. doi: 10.1016/j.cell.2013.07.030
53. Pearce EJ, Everts B. Dendritic cell metabolism. *Nat Rev Immunol.* (2015) 15:18–29. doi: 10.1038/nri3771
54. O'Neill LA. A critical role for citrate metabolism in LPS signalling. *Biochem J.* (2011) 438:e5–6. doi: 10.1042/BJ20111386
55. Wculek S, Sofia Khoulili C, Elena P, Heras-Murillo I, David S. Metabolic control of dendritic cell functions: digesting information. *Front Immunol.* (2019) 10:775. doi: 10.3389/fimmu.2019.00775
56. Fekete T, Suto MI, Bencze D, Mazlo A, Szabo A, Biro T, et al. Human plasmacytoid and monocyte-derived dendritic cells display distinct metabolic profile upon rig-i activation. *Front Immunol.* (2018) 9:3070. doi: 10.3389/fimmu.2018.03070
57. McWilliams TG, Prescott AR, Montava-Garriga L, Ball G, Singh F, Barini E, et al. Basal mitophagy occurs independently of PINK1 in mouse tissues of high metabolic demand. *Cell Metab.* (2018) 27:439–49.e5. doi: 10.1016/j.cmet.2017.12.008
58. Vats D, Mukundan L, Odegaard JI, Zhang L, Smith K, Morel CR, et al. Oxidative metabolism and PGC-1beta attenuate macrophage-mediated inflammation. *Cell Metab.* (2006) 4:13–24. doi: 10.1016/j.cmet.2006.05.011
59. Bell C, English L, Boulais J, Chemali M, Caron-Lizotte O, Desjardins M, et al. Quantitative proteomics reveals the induction of mitophagy in tumor necrosis factor-alpha-activated (TNFalpha) macrophages. *Mol Cell Proteomics.* (2013) 12:2394–407. doi: 10.1074/mcp.M112.025775
60. Mauro-Lizcano M, Esteban-Martinez L, Seco E, Serrano-Puebla A, Garcia-Ledo L, Figueiredo-Pereira C, et al. New method to assess mitophagy flux by flow cytometry. *Autophagy.* (2015) 11:833–43. doi: 10.1080/15548627.2015.1034403
61. Petit A, Kawarai T, Paitel E, Sanjo N, Maj M, Scheid M, et al. Wild-type PINK1 prevents basal and induced neuronal apoptosis, a protective effect abrogated by Parkinson disease-related mutations. *J Biol Chem.* (2005) 280:34025–32. doi: 10.1074/jbc.M505143200
62. Klinkenberg M, Thurow N, Gispert S, Ricciardi F, Eich F, Prehn J, et al. Enhanced vulnerability of PARK6 patient skin fibroblasts to apoptosis induced by proteasomal stress. *Neuroscience.* (2010) 166:422–34. doi: 10.1016/j.neuroscience.2009.12.068
63. Liu W, Acin-Perez R, Geggman KD, Manfredi G, Lu B, Li C. Pink1 regulates the oxidative phosphorylation machinery via mitochondrial fission. *Proc Natl Acad Sci USA.* (2011) 108:12920–4. doi: 10.1073/pnas.1107332108
64. Morais VA, Verstreken P, Roethig A, Smet J, Snellinx A, Vanbrabant M, et al. Parkinsons disease mutations in PINK1 result in decreased Complex I activity and deficient synaptic function. *EMBO Mol Med.* (2009) 1:99–111. doi: 10.1002/emmm.200900006
65. Gegg ME, Cooper JM, Schapira AH, Taanman JW. Silencing of PINK1 expression affects mitochondrial DNA and oxidative phosphorylation in dopaminergic cells. *PLoS ONE.* (2009) 4:e4756. doi: 10.1371/journal.pone.0004756
66. Amo T, Sato S, Saiki S, Wolf AM, Toyomizu M, Gautier CA, et al. Mitochondrial membrane potential decrease caused by loss of PINK1 is not due to proton leak, but to respiratory chain defects. *Neurobiol Dis.* (2011) 41:111–8. doi: 10.1016/j.nbd.2010.08.027
67. Requejo-Aguilar R, Lopez-Fabuel I, Fernandez E, Martins LM, Almeida A, Bolaños JP. PINK1 deficiency sustains cell proliferation by reprogramming glucose metabolism through HIF1. *Nat Commun.* (2014) 5:4514. doi: 10.1038/ncomms5514
68. Everts B, Pearce EJ. Metabolic control of dendritic cell activation and function: recent advances and clinical implications. *Front Immunol.* (2014) 5:203. doi: 10.3389/fimmu.2014.00203
69. Wang X, Winter D, Ashrafi G, Schlehe J, Wong YL, Selkoe D, et al. PINK1 and Parkin target Miro for phosphorylation and degradation to arrest mitochondrial motility. *Cell.* (2011) 147:93–906. doi: 10.1016/j.cell.2011.10.018
70. Tosukhpong P, Boonla C, Dissayabutra T, Kaewwilai L, Muen Sri S, Chotipanich C, et al. Biochemical and clinical effects of whey protein supplementation in Parkinsons disease: a pilot study. *J Neurol Sci.* (2016) 367:162–70. doi: 10.1016/j.jns.2016.05.056
71. Course MM, Scott AI, Schoor C, Hsieh CH, Papakyrikos AM, Winter D, et al. Phosphorylation of MCAD selectively rescues PINK1 deficiencies in behavior and metabolism. *Mol Biol Cell.* (2018) 29:1219–27. doi: 10.1091/mbc.E18-03-0155
72. Crown SB, Marze N, Antoniewicz M R. Catabolism of branched chain amino acids contributes significantly to synthesis of odd-chain and even-chain fatty acids in 3T3-L1 adipocytes. *PLoS ONE.* (2015) 10:e0145850. doi: 10.1371/journal.pone.0145850
73. Tang JE, Moore DR, Kujbida GW, Tarnopolsky M, Phillips SM. Ingestion of whey hydrolysate, casein, or soy protein isolate: effects on mixed muscle protein synthesis at rest and following resistance exercise in young men. *J Appl Physiol.* (2009) 107:987–92. doi: 10.1152/jappphysiol.00076.2009
74. Rawat AK, Korthikunta V, Gautam S, Pal S, Tadigoppula N, Tamrakar A, et al. 4-Hydroxyisoleucine improves insulin resistance by promoting mitochondrial biogenesis and act through AMPK and Akt dependent pathway. *Fitoterapia.* (2014) 99:307–17. doi: 10.1016/j.fitote.2014.10.006
75. Schnuck JK, Sunderland KL, Gannon NP, Kuennen M, Vaughan RA. Leucine stimulates PPARbeta/delta-dependent mitochondrial biogenesis and oxidative metabolism with enhanced GLUT4 content and glucose uptake in myotubes. *Biochimie.* (2016) 128–129:1–7. doi: 10.1016/j.biochi.2016.06.009
76. Sun X, Zemel MB. Leucine modulation of mitochondrial mass and oxygen consumption in skeletal muscle cells and adipocytes. *Nutr Metab.* (2009) 56:26. doi: 10.1186/1743-7075-6-26
77. O'Neill HM, Holloway GP, Steinberg GR. AMPK regulation of fatty acid metabolism and mitochondrial biogenesis: implications for obesity. *Mol Cell Endocrinol.* (2013) 366:135–51. doi: 10.1016/j.mce.2012.06.019
78. Haruta T, Uno T, Kawahara J, Takano A, Egawa K, Sharma P, et al. A rapamycin-sensitive pathway down-regulates insulin signaling via phosphorylation and proteasomal degradation of insulin receptor substrate-1. *Mol Endocrinol.* (2000) 14:783–94. doi: 10.1210/mend.14.6.0446

79. Laplante M, Sabatini DM. mTOR signaling in growth control and disease. *Cell*. (2012) 149:274–93. doi: 10.1016/j.cell.2012.03.017
80. Ibrahim J, Nguyen AH, Rehman A, Ochi A, Jamal M, Graffeo CS, et al. Dendritic cell populations with different concentrations of lipid regulate tolerance and immunity in mouse and human liver. *Gastroenterology*. (2012) 143:1061–72. doi: 10.1053/j.gastro.2012.06.003
81. Choi J, Ravipati A, Nimmagadda V, Schubert M, Castellani RJ, Graffeo CS. Potential roles of PINK1 for increased PGC-1alpha-mediated mitochondrial fatty acid oxidation and their associations with Alzheimer disease and diabetes. *Mitochondrion*. (2014) 18:41–8. doi: 10.1016/j.mito.2014.09.005
82. Maroof A, English NR, Bedford PA, Gabrilovich D, Knight SC. Developing dendritic cells become lacy cells packed with fat and glycogen. *Immunology*. (2005) 115:473–83. doi: 10.1111/j.1365-2567.2005.02181.x
83. Kim J, Byun JW, Choi I, Kim B, Jeong H, Jou I, et al. PINK1 deficiency enhances inflammatory cytokine release from acutely prepared brain slices. *Exp Neurol*. (2013) 22:38–44. doi: 10.5607/en.2013.22.1.38
84. Sliter DA, Martinez J, Hao L, Chen X, Sun N, Fischer T, et al. Parkin and PINK1 mitigate STING-induced inflammation. *Nature*. (2018) 561:258–62. doi: 10.1038/s41586-018-0448-9
85. Matheoud D, Sugiura A, Bellemare-Pelletier A, Laplante A, Rondeau C, Chemali M, et al. Parkinsons disease-related proteins PINK1 and Parkin repress mitochondrial antigen presentation. *Cell*. (2016) 166:314–27. doi: 10.1016/j.cell.2016.05.039

Conflict of Interest: The authors declare that the research was conducted in the absence of any commercial or financial relationships that could be construed as a potential conflict of interest.

Copyright © 2019 Basit and de Vries. This is an open-access article distributed under the terms of the Creative Commons Attribution License (CC BY). The use, distribution or reproduction in other forums is permitted, provided the original author(s) and the copyright owner(s) are credited and that the original publication in this journal is cited, in accordance with accepted academic practice. No use, distribution or reproduction is permitted which does not comply with these terms.